



# Energetic performance is improved by specific activation of $K^+$ fluxes through $K_{Ca}$ channels in heart mitochondria

Miguel A. Aon<sup>a</sup>, Sonia Cortassa<sup>a</sup>, An-Chi Wei<sup>a</sup>, Morten Grunnet<sup>b</sup>, Brian O'Rourke<sup>a,\*</sup>

<sup>a</sup> The Johns Hopkins University, School of Medicine, Institute of Molecular Cardiology, 720 Rutland Ave., 1060 Ross Bldg., Baltimore, MD 21205-2195, USA

<sup>b</sup> Department of Biomedical Sciences, The Danish National Research Foundation Center for Cardiac Arrhythmia, University of Copenhagen, the Panum Institute, Copenhagen, Denmark, and NeuroSearch A/S, Ballerup, Denmark

## ARTICLE INFO

### Article history:

Received 16 July 2009

Received in revised form 27 August 2009

Accepted 31 August 2009

Available online 8 September 2009

### Keywords:

Mitochondrial volume

Membrane potential

Respiratory control ratio

Valinomycin

P/O ratio

$K_{Ca}$  activator

## ABSTRACT

Mitochondrial volume regulation depends on  $K^+$  movement across the inner membrane and a mitochondrial  $Ca^{2+}$ -dependent  $K^+$  channel (mito $K_{Ca}$ ) reportedly contributes to mitochondrial  $K^+$  uniporter activity. Here we utilize a novel  $K_{Ca}$  channel activator, NS11021, to examine the role of mito $K_{Ca}$  in regulating mitochondrial function by measuring  $K^+$  flux, membrane potential ( $\Delta\Psi_m$ ), light scattering, and respiration in guinea pig heart mitochondria.  $K^+$  uptake and the influence of anions were assessed in mitochondria loaded with the  $K^+$  sensor PBFI by adding either the chloride (KCl), acetate (KAc), or phosphate ( $KH_2PO_4$ ) salts of  $K^+$  to energized mitochondria in a sucrose-based medium.  $K^+$  fluxes saturated at  $\sim 10$  mM for each salt, attaining maximal rates of  $172 \pm 17$ ,  $54 \pm 2.4$ , and  $33 \pm 3.8$  nmol  $K^+$ /min/mg in KCl, KAc, or  $KH_2PO_4$ , respectively. NS11021 (50 nM) increased the maximal  $K^+$  uptake rate by 2.5-fold in the presence of  $KH_2PO_4$  or KAc and increased mitochondrial volume, with little effect on  $\Delta\Psi_m$ . In KCl, NS11021 increased  $K^+$  uptake by only 30% and did not increase volume. The effects of NS11021 on  $K^+$  uptake were inhibited by the  $K_{Ca}$  toxins charybdotoxin (200 nM) or paxilline (1  $\mu$ M). Fifty nanomolar of NS11021 increased the mitochondrial respiratory control ratio (RCR) in  $KH_2PO_4$ , but not in KCl; however, above 1  $\mu$ M, NS11021 decreased RCR and depolarized  $\Delta\Psi_m$ . A control compound lacking  $K_{Ca}$  activator properties did not increase  $K^+$  uptake or volume but had similar nonspecific (toxin-insensitive) effects at high concentrations. The results indicate that activating  $K^+$  flux through mito $K_{Ca}$  mediates a beneficial effect on energetics that depends on mitochondrial swelling with maintained  $\Delta\Psi_m$ .

© 2009 Elsevier B.V. All rights reserved.

## 1. Introduction

Increased mitochondrial volume and an improvement in oxidative phosphorylation have been implicated in the mechanism of ischemic or pharmacological preconditioning [1,2], but the links between altered  $K^+$  flux and the functional effects are not well understood [3,4].  $K^+$  is the principal monovalent cation in the cytoplasm and, owing to the large electrochemical driving force, is consequently an important ion mediating changes in volume when the  $K^+$  conductance of the inner membrane is altered. Because of the restricted matrix space, the mitochondria have been referred to as “perfect osmometers,” hence, the coordinated uptake of both cations and anions, along with water, mediates swelling [4]. Early work stressed the existence of selective electrophoretic pathways for cation uptake and anion transport associated with mitochondrial swelling [5,6], and Garlid et al. [1] have provided supporting evidence that the major volume regulation involves  $K^+$  cycling, consisting of electrophoretic  $K^+$  influx and electroneutral  $K^+$  efflux by the  $K^+$ /H<sup>+</sup> exchanger.

Although electroneutral,  $K^+$  extrusion via  $K^+$ /H<sup>+</sup> antiporter requires the proton gradient [7].

The interaction between mitochondrial volume changes and altered energetics in the context of cardioprotection is unclear and currently under debate [1,2,8]. At least three interdependent regulatory processes may be involved, including i)  $K^+$  uptake, ii) matrix volume changes, and iii) mitochondrial energetic alterations (involving respiration,  $\Delta\Psi_m$ , and the NADH produced by the TCA cycle). Enhanced mitochondrial  $K^+$  influx through ATP-dependent (mito $K_{ATP}$ ) [9] or  $Ca^{2+}$ -dependent (mito $K_{Ca}$ )  $K^+$  channels has been proposed as a potential mediator of protection, and the concomitant increase in mitochondrial volume could alter electron flow through the respiratory chain [10,11]. In this regard, it has been proposed that the increase in matrix volume may enhance ATP/ADP exchange with the cytoplasm by bringing the inner and outer mitochondrial membranes closer together [1,2,8].

Increases in cytoplasmic  $Ca^{2+}$  during excitation-contraction coupling or hormonal stimulation result in an increase in mitochondrial matrix  $Ca^{2+}$  and this is an important factor regulating oxidative phosphorylation. Davidson and Halestrap [12] and Halestrap [13] reported that matrix  $Ca^{2+}$  inhibits a pyrophosphatase, resulting in a rise in matrix pyrophosphate and stimulation of  $K^+$  influx in liver or heart

\* Corresponding author. Tel.: +1 410 614 0034; fax: +1 410 502 5055.

E-mail address: [bor@jhmi.edu](mailto:bor@jhmi.edu) (B. O'Rourke).

mitochondria. Alternatively, Brown and Brand [14] proposed a  $\text{Ca}^{2+}$ -mediated increase in matrix volume operating through the well-known activating effect of  $\text{Ca}^{2+}$  on tricarboxylic acid cycle dehydrogenases, in turn stimulating respiration and increasing  $\Delta\Psi_m$ , thus increasing the electrochemical driving force for  $\text{K}^+$  uniport activity [10,14]. More recently, we proposed that elevated matrix  $\text{Ca}^{2+}$  could open large conductance  $\text{Ca}^{2+}$ -activated  $\text{K}^+$  channels present in the inner membrane of cardiac mitochondria [15]. Similarly,  $\text{K}_{\text{Ca}}$ -type channels have been reported in mitochondria from brain [16–18] and cultured human glioma cells [19]. However, the nonspecific effects of high concentrations of  $\text{K}_{\text{Ca}}$  activators (e.g., NS1619) on mitochondrial energetics [20,21] have complicated interpretation of the role of  $\text{mitoK}_{\text{Ca}}$  in cardioprotection.

In the present work, we examine the effects of a novel, more potent,  $\text{K}_{\text{Ca}}$  channel opener NS11021 [22] and its inactive form (NS13558) on mitochondrial  $\text{K}^+$  fluxes, matrix volume, and  $\Delta\Psi_m$  in energized mitochondria and also evaluate their impact on mitochondrial respiration. We show that in the nanomolar concentration range, NS11021 accelerates the initial rate of  $\text{K}^+$  uptake and potentiates mitochondrial swelling in the presence of permeable anions, while in the micromolar range, it leads to energetic deterioration. The beneficial effects correlate with expansion of the matrix space and are sensitive to the  $\text{K}_{\text{Ca}}$  channel inhibitors charybdotoxin or paxilline, while the nonspecific effects are not. Moreover, the control compound does not recapitulate the effects of NS11021 on  $\text{K}^+$  uptake or volume but does reproduce the toxin-insensitive nonspecific actions.

## 2. Materials and methods

### 2.1. Mitochondrial isolation from guinea pig hearts

The protocol of mitochondrial isolation for a small sample tissue (2–4 g of fresh tissue) described in Mela and Seitz [23] was followed with slight modifications. Briefly, a 300 g weight guinea pig was euthanized and the heart was quickly excised. After harvesting the heart, the whole procedure was performed on ice. The heart was immediately immersed into ~10 ml of isolation solution (IS) consisting of 75 mM sucrose, 225 mM mannitol, and 0.01 mM EGTA neutralized with Trizma buffer at pH 7.4. After washing, the top of the heart corresponding to the aorta, the pulmonaries, and the atria were discarded, and immersed into fresh 20 ml of IS and minced. After the tissue pieces settled, the entire supernatant was discarded and fresh IS (5 ml) was added, and the mixture was transferred to a hand homogenizer. Proteinase (0.8 mg, bacterial, type XXIV, Sigma, formerly called Nagarse) was added just before starting the homogenization procedure. The whole homogenization procedure took no longer than 14 min in two steps of ~7 min (each with 5 ml addition of fresh IS). The homogenate was carefully transferred after each step to a polycarbonate centrifuge tube. After 5 min of  $480\times g$  of centrifugation to discard unbroken tissue and debris, the supernatant was centrifuged at  $7700\times g$  for 10 min to sediment the mitochondria. The mitochondrial pellet was washed twice with IS and the last one with suspension solution (IS without EGTA) at  $7700\times g$  for 5 min each. An average of 10 mg mitochondrial protein/ml was obtained from one guinea pig heart with this procedure.

Respiratory control ratios (RCRs; ratio of state 3 over state 4 respiration with glutamate + malate as the substrate) of 10 to 20 were obtained using this method (see Fig. 1). The quality of the mitochondrial preparation was confirmed using electron microscopy. Electron micrographs showed that the Nagarse method yielded a more representative sample of mitochondria with less damage and fragmentation, as confirmed by isolating mitochondria simultaneously from two halves of the same heart in the presence or in the absence of Nagarse (data not shown).

Mitochondrial protein was determined using the bicinchonic acid method, BCA™ protein assay kit (Pierce, IL).

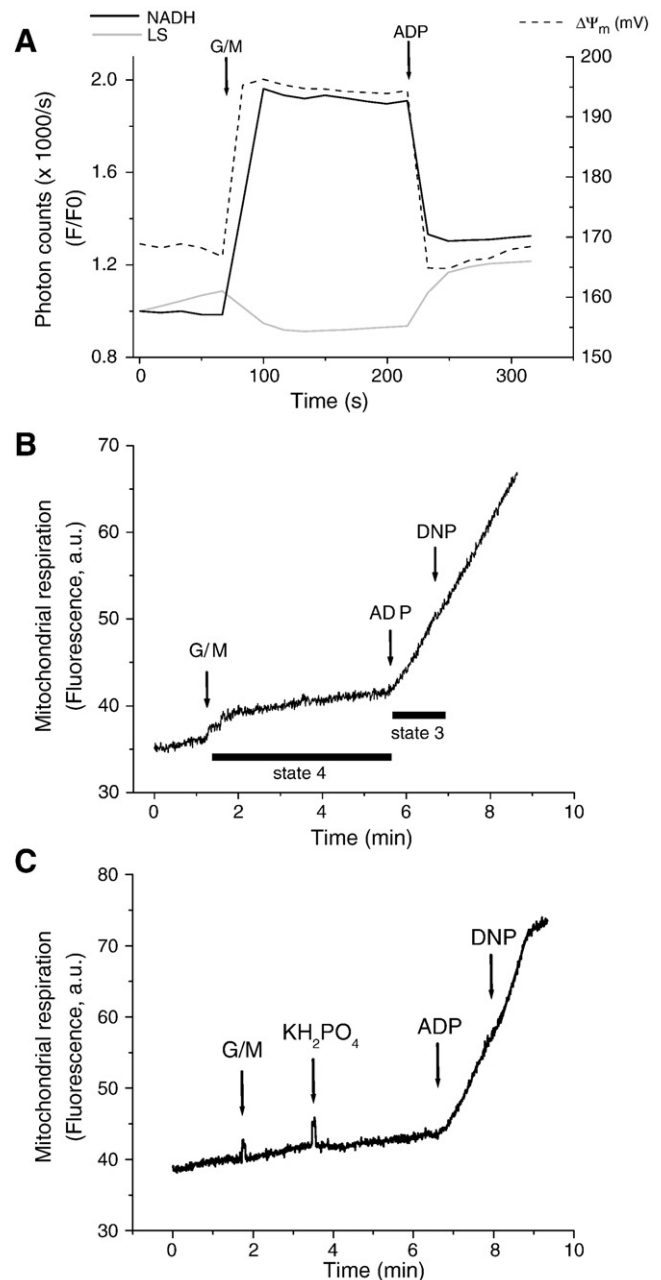


**Fig. 1.** Simultaneous monitoring of mitochondrial volume,  $\Delta\Psi_m$ , and NAD(P)H, and respiration during state 4 and the state 4→state 3 transition in isolated guinea pig heart mitochondria. (A) Freshly isolated mitochondria from guinea pig heart were resuspended (~100  $\mu\text{g}$  mitochondrial protein) in the cuvette of a spectrofluorometer containing 2 ml isotonic sucrose-based assay medium in the presence of 100 nM TMRM with constant stirring at 37 °C. At the indicated times, 5 mM glutamate- $\text{Na}^+$ /malate- $\text{Na}^+$  (first arrow) or 1 mM ADP (second arrow) was added. (B, C) Mitochondrial respiration was assayed in a respirometer as described in the [Materials and methods](#) section. An increase in signal represents a decrease in oxygen in the chamber. The uncoupler DNP (50  $\mu\text{M}$ ) was added to determine maximal uncoupled respiration. In panel C, a representative trace is depicted corresponding to mitochondria pre-incubated with 50 nM NS11021, energized with G/M, and subjected to a pulse of 20 mM  $\text{KH}_2\text{PO}_4$ . Notice the decrease in state 4 respiration due to activation of  $\text{K}^+$  fluxes and swelling (see [Figs. 3B and 4](#)). In panel A, it can be clearly seen that on substrate addition, mitochondria respond with low-amplitude swelling (gray trace),  $\Delta\Psi_m$  polarization by ~40 mV (dashed trace) and a 2-fold NAD(P)H pool reduction (black trace) whereas ADP addition has the opposite effect, i.e. a volume decrease,  $\Delta\Psi_m$  depolarization, and NAD(P)H oxidation. Similar results were obtained in isotonic 137 mM KCl-based medium. Key to abbreviations: G/M, glutamate- $\text{Na}^+$ /malate- $\text{Na}^+$ ; DNP, dinitrophenol.

## 2.2. Assay of mitochondrial activity

Mitochondrial respiration was assayed at 37 °C in a closed chamber of 0.35 ml containing (in mM): 250 sucrose (or 137 KCl), 2  $\text{KH}_2\text{PO}_4$ , 0.5 EGTA, 2.5  $\text{MgCl}_2$ , 20 HEPES at pH 7.1, and 100 to 200  $\mu\text{g}$  of mitochondrial protein. The  $\text{O}_2$  concentration in the chamber was monitored by means of a fiber optic  $\text{O}_2$  sensor (Ocean Optics, Inc; probe tip diameter = 1 mm) in which the fluorescence emission at 600 nm of a ruthenium compound is quenched by  $\text{O}_2$ . The fluorescence signal was calibrated using different mixtures of  $\text{O}_2$  and  $\text{N}_2$  and was linear in the range 1%–60%  $\text{O}_2$ . To calculate the ATP/O ratio, aliquots of 100  $\mu\text{M}$  of ADP were added and the difference between the  $\text{O}_2$  signal recorded before and after the ADP addition was quantified upon return to state 4 (i.e., when all of the ADP was converted to ATP).

Mitochondrial swelling,  $\Delta\Psi_m$ , and NAD(P)H were monitored simultaneously with a spectrofluorometer (Photon Technology, Inc.) in an experimental solution containing (in mM): 250 sucrose (or 137 KCl), 0.5 EGTA, 2.5  $\text{MgCl}_2$ , 20 HEPES, pH 7.1. Mitochondrial swelling was measured as a decrease in the 90° light scattering signal using 520 nm excitation [24–26].  $\Delta\Psi_m$  was recorded using tetramethylrhodamine methyl ester (TMRM; 100 nM) and applying the ratiometric method of Scaduto and Grotyohann [27]. Briefly, this

method uses two excitation wavelengths ( $\lambda_{\text{exc}}$ ) at 546 nm and 573 nm while recording the fluorescence emission ( $\lambda_{\text{em}}$ ) at 590 nm. A calibration curve of  $\Delta\Psi_m$  versus the 573/546 nm ratio was constructed to estimate  $\Delta\Psi_m$  in each experiment. PBFI fluorescence was monitored ratiometrically (340/380 nm excitation at 495 nm emission; see also next subsection) and NAD(P)H fluorescence was measured at  $\lambda_{\text{em}} = 450$  nm with  $\lambda_{\text{exc}} = 340$  nm.

## 2.3. Measurement of $\text{K}^+$ uptake in heart mitochondria

Freshly isolated mitochondria were loaded with 20  $\mu\text{M}$  PBFI-AM for 20 min at room temperature with occasional shaking. Excess dye was removed by centrifugation (1.5 min at 14,000 $\times g$ ), and the mitochondrial pellet was washed once under the same centrifugation conditions. After resuspension in 225 mM mannitol and 75 mM sucrose, mitochondria were assayed for  $\text{K}^+$  uptake in the same medium described for the respiration measurements with the exception that 250 mM sucrose was used instead of 137 mM KCl. This allowed us to study the initial  $\text{K}^+$  uptake rate in a controlled fashion. In order to relate the increase in the 340/380 nm ratio of PBFI fluorescence to  $\text{K}^+$  concentration, 1  $\mu\text{M}$  of PBFI salt was dissolved in the same assay medium, but in the absence of mitochondria. The

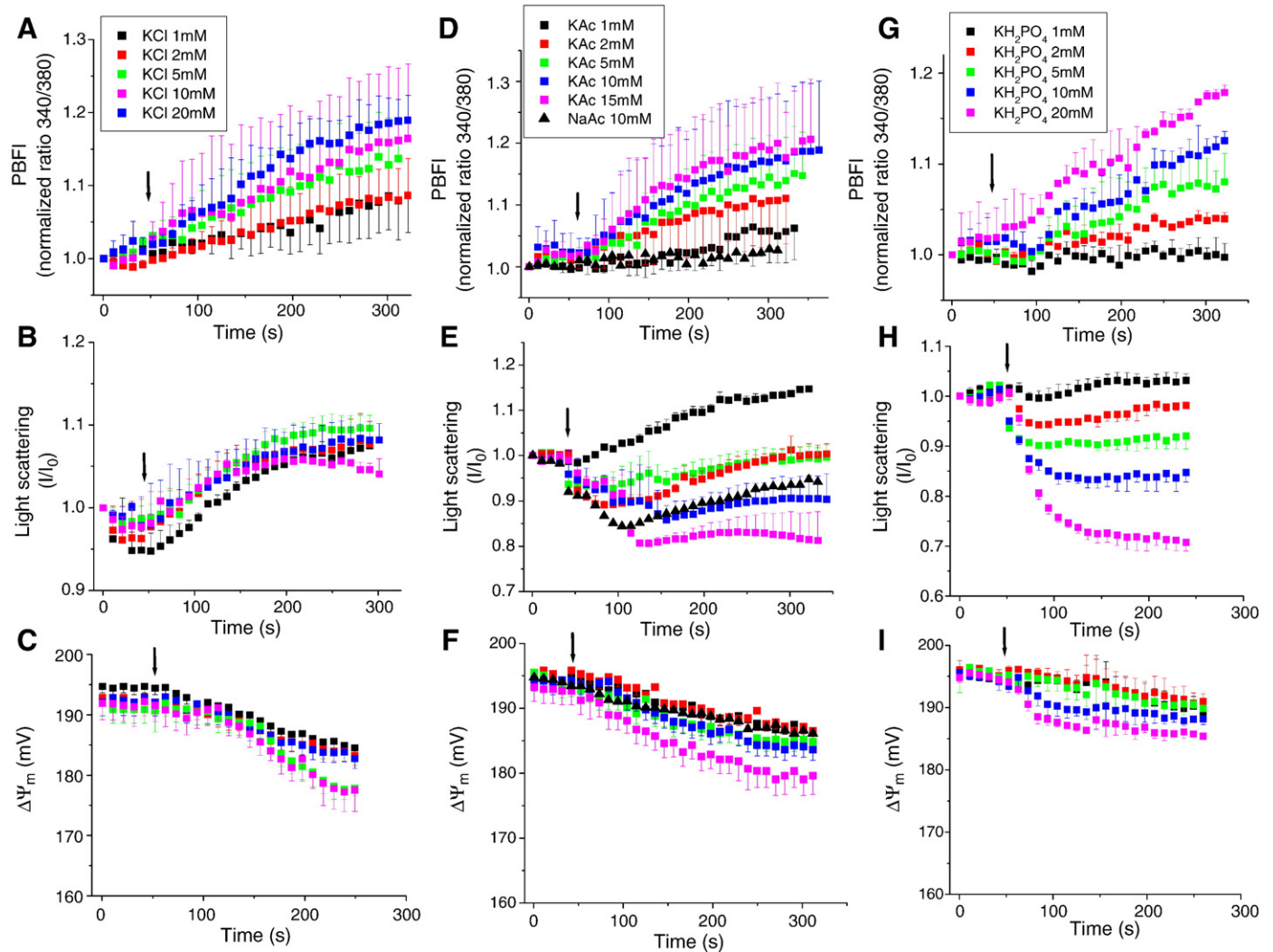


**Fig. 2.** Simultaneous monitoring of  $\text{K}^+$  fluxes, volume, and  $\Delta\Psi_m$ , following pulses of different  $\text{K}^+$  salts in isolated mitochondria. Freshly isolated mitochondria from guinea pig heart, resuspended and assayed as described in the legend of Fig. 1, were energized with 5 mM G/G (both  $\text{Na}^+$  neutralized) in isosmotic sucrose-based medium. Under these state 4 respiration conditions, different concentrations of potassium chloride, KCl (A–C), potassium acetate, KAc (D–F), or potassium phosphate  $\text{KH}_2\text{PO}_4$  (G–I) were added, and the normalized PBFI fluorescence ratio 340/380 (A, D, G), 90° light scattering (B, E, H), and  $\Delta\Psi_m$  (C, F, I) were simultaneously monitored. The results obtained from two independent experiments are shown. Arrows point to the time of the  $\text{K}^+$  salt addition.



increase in PBFI ratio was determined as a function of increasing concentrations of KCl, KAc, or  $\text{KH}_2\text{PO}_4$ . The conversion factor for each of the  $\text{K}^+$  salts was obtained from the slope of the plot of PBFI ratio vs  $\text{K}^+$  concentration.

#### 2.4. Determination of mitochondrial volume

We used the radioactive tracer method to measure mitochondrial volume [28,29], in order to further quantify  $\text{K}^+$  fluxes. This method uses  $^3\text{H}$ -labeled water ( $^3\text{H}_2\text{O}$ ) and  $^{14}\text{C}$ -labeled mannitol ( $^{14}\text{C}$  mannitol). Mitochondrial volume was determined in four replicates for each  $\text{K}^+$  salt under the same conditions as the fluorometric experiments measuring  $\text{K}^+$  uptake. Using the kinetics of mitochondrial volume change as determined by  $90^\circ$  light scattering, we sampled mitochondria before and after addition of the  $\text{K}^+$  salt for the volume determination. Briefly,  $1 \mu\text{Ci}$  of  $^3\text{H}_2\text{O}$  and  $0.2 \mu\text{Ci}$  of  $^{14}\text{C}$  Mannitol were added to  $0.5 \text{ ml}$  of mitochondrial suspension ( $2$  to  $3 \text{ mg}$  of mitochondrial protein/ $\text{ml}$ ), and incubated for  $3 \text{ min}$ . After incubation, the whole volume was transferred to a microcentrifuge tube and centrifuged at  $13,000 \times g$  for  $3 \text{ min}$ . The whole volume of the supernatant was recovered and counted, and the pellet was dissolved with  $0.1 \text{ ml}$  of perchloric acid  $20\%$  (wt./wt.) and also counted (Beckman LS 6000, Beckman Instruments Inc., Fullerton CA).

Several controls were performed in order to account for i) count spillover: mitochondria were incubated with one radioactive tracer at a time, centrifuged, and supernatant and pellet counted in the  $^{14}\text{C}$  and  $^3\text{H}$  channels in duplicate; ii) nonspecific binding of  $^{14}\text{C}$  mannitol: mitochondria were subjected to osmotic lysis, and the same centrifugation as well as counting protocol was followed; and iii) quenching of the  $^{14}\text{C}$  and  $^3\text{H}$  tracers introduced by perchloric acid:  $0.01 \mu\text{Ci}$  of each radioactive tracer was dissolved in  $0.5 \text{ ml}$  of water; half of the volume was acidified with perchloric acid whereas the other half was counted directly.

#### 2.5. Electron microscopy of mitochondria

The electron microscopy of freshly isolated mitochondria was performed at The Johns Hopkins University School of Medicine Microscope Facility using standard procedures. Briefly, immediately after isolation, an aliquot of mitochondrial suspension ( $0.6$ – $0.8 \text{ mg}$  of mitochondrial protein) was fixed in  $2\%$  glutaraldehyde,  $2\%$  formaldehyde with  $3 \text{ mM}$   $\text{CaCl}_2$  in  $0.1 \text{ M}$  cacodylate buffer for  $1 \text{ h}$  at room temperature. After washing in  $0.1 \text{ M}$  cacodylate buffer, the pellet was post-fixed in reduced osmium tetroxide for  $1 \text{ h}$  at  $4^\circ\text{C}$ . Pre-embed staining was done with  $2\%$  uranyl acetate in  $\text{dH}_2\text{O}$ . The pellet was then dehydrated in graded ethanol and embedded in Eponate 12 from Ted Pella. Thin sections were cut on a Reichert-Jung Ultracut E microtome and placed on  $200$  mesh copper grids. The grids were post-stained with uranyl acetate followed by lead citrate and viewed on a Hitachi 7600 TEM. Digital images were collected with an AMT Advantage HR side mount camera.

##### 2.5.1. Data reproducibility and statistical analysis

All representative records shown in this paper were confirmed in at least three independent experiments. Data were analyzed with the software GraphPad Prism (Ver. 3; San Diego, CA) or MicroCal Origin. The statistical significance of the differences between treatments was evaluated with ANOVA using Tukey's multiple comparison test, and the results presented as the mean  $\pm$  SEM (95% confidence interval).

#### 2.6. Materials

NS11021 (1-(3,5-bis-trifluoromethyl-phenyl)-3-(4-bromo-2-(1H-tetrazol-5-yl)-phenyl)-thiourea) and its inactive form NS13558 (a  $-\text{CH}_3$  added to the tetrazole moiety of NS11021) were a generous

gift from NeuroSearch A/S (Denmark). Paxilline was obtained from Biomol International and charybdotoxin recombinant *Escherichia coli* from Calbiochem (La Jolla, CA). The acetoxymethyl (AM) ester form of the  $\text{K}^+$ -sensitive benzofuran isophthalate (PBFI), and tetramethylrhodamine methyl ester (TMRM), were purchased from Invitrogen (Carlsbad, CA). All other reagents were purchased from Sigma.

### 3. Results

Freshly isolated mitochondria from guinea pig heart were resuspended in an isotonic sucrose-based assay medium, and energized with  $5 \text{ mM}$  each of glutamate- $\text{Na}^+$ /malate- $\text{Na}^+$  (G/M). The attainment of state 4 was assessed by simultaneous monitoring of  $\Delta\Psi_m$ , NADH, and swelling ( $90^\circ$  light scattering) after addition of G/M. In isotonic sucrose medium ( $250 \text{ mOsm}$ ),  $\Delta\Psi_m$  increased immediately by  $\sim 30$ – $50 \text{ mV}$  in parallel with reduction of the NADH pool, and low-amplitude swelling (Fig. 1A). On ADP ( $1 \text{ mM}$ ) addition, the mitochondria exhibit the state  $4 \rightarrow$  state 3 transition associated with  $\Delta\Psi_m$  depolarization ( $\sim 30 \text{ mV}$ ), NADH oxidation, and contraction. Similar changes occurred in KCl-based isotonic medium (data not

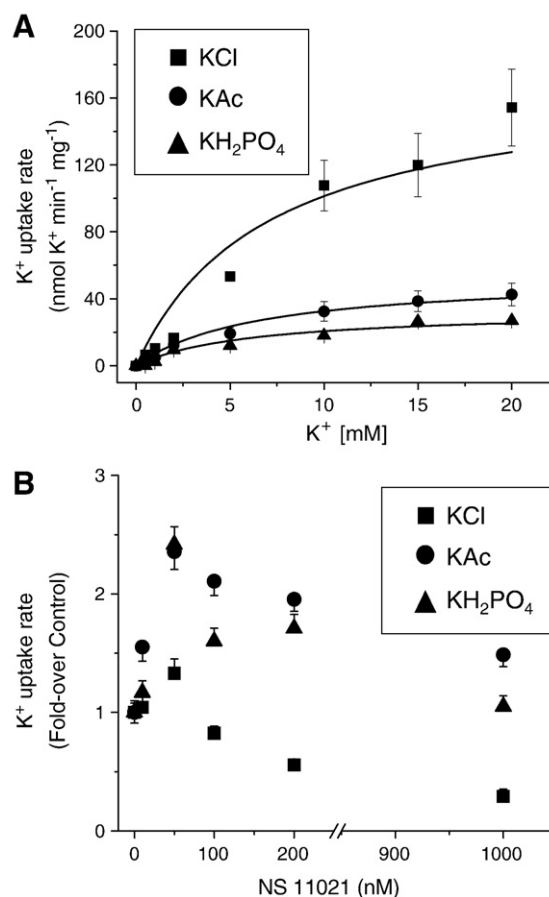


**Fig. 3.** Kinetics of  $\text{K}^+$  uptake and its activation by NS11021 in isolated mitochondria from guinea pig heart. (A) The initial rates of  $\text{K}^+$  uptake (nmol  $\text{K}^+$ /min/mg) after pulses of KCl, KAc, or  $\text{KH}_2\text{PO}_4$ , at different concentrations, were quantified from traces like those shown in Fig. 2 (panels A, D, G). Each point in the plot is the result obtained from three independent mitochondrial isolations. The kinetic parameters  $K_{0.5}$  and  $V_{\text{max}}$  were obtained after non-linear regression analysis according to a Michaelis-Menten type of expression ( $V = V_{\text{max}}(S)/(K_{0.5} + (S))$ ) performed in MicroCal Origin. The PBFI ratio 340/380 was related to  $\text{K}^+$  concentration as described in the Materials and methods section. (B) The initial rates of  $\text{K}^+$  uptake after addition of  $10 \text{ mM}$  KCl, KAc, or  $\text{KH}_2\text{PO}_4$ , to state 4 mitochondria in the absence (control) or the presence of  $10 \text{ nM}$ ,  $50 \text{ nM}$ ,  $100 \text{ nM}$ ,  $200 \text{ nM}$ , or  $1 \mu\text{M}$  of NS11021. The PBFI ratio,  $90^\circ$  light scattering, and  $\Delta\Psi_m$  were monitored simultaneously.  $\text{K}^+$  fluxes normalized to the control (absence of NS11021) for each  $\text{K}^+$  salt are shown (two independent experiments).

shown). Independent measurements of mitochondrial respiration following an identical protocol showed an abrupt increase in oxygen consumption following ADP addition in the presence of G/M (Fig. 1B). These observations are in accord with published experimental evidence (e.g., [30,31]).

### 3.1. $K^+$ uptake in heart mitochondria

$K^+$  uptake was assessed with mitochondria in state 4 (i.e., after energization with 5 mM G/M but in the absence of ADP) after the addition of different  $K^+$  salts. From first principles, due to the limitations imposed by charge balance, mitochondrial swelling can only occur when both cations and anions are permeable to the mitochondrial inner membrane [5,32]. Thus,  $K^+$  uptake was assessed in the presence of the relatively impermeable  $Cl^-$  [33,34], the passively diffusing  $Ac^-$  [35], and the carrier-mediated  $H_2PO_4^-$  [36].

We used the  $K^+$ -sensitive ratiometric fluorescent dye PBFI to directly and quantitatively measure  $K^+$  fluxes in isolated mitochondria. Mitochondria were incubated in the presence of 5 mM G/M in isotonic sucrose medium and different concentrations of each potassium salt were added to the cuvette. A reproducible increase in PBFI fluorescence (ratio 340/380) could be detected in mitochondria when subjected to additions of increasing concentrations of KCl (Fig. 2A), KAc (Fig. 2D), and  $KH_2PO_4$  (Fig. 2G). As shown in Fig. 3A,  $K^+$  fluxes saturated above 10 mM for each salt and attained maximal rates (in nmol  $K^+$ /min/mg) of  $172 \pm 17$ ,  $54 \pm 2.4$ , and  $33 \pm 3.8$  in KCl,

KAc, and  $KH_2PO_4$ , respectively. The  $K_{0.5}$  was similar in all three cases (in mM):  $7 \pm 0.9$ ,  $6.4 \pm 0.5$ , and  $6.0 \pm 0.6$ , respectively.

The specificity of the response of the  $K^+$ -sensitive probe was assessed by subjecting mitochondria to an addition of 10 mM  $Na^+$  acetate (NaAc, Fig. 2D). Under conditions in which 10 mM KAc gave a clear increase in PBFI fluorescence, no increase could be registered with 10 mM NaAc (Fig. 2D), verifying the  $K^+$  selectivity of the PBFI. However, a decrease in the light scattering signal occurred after either 10 mM KAc or NaAc, indicating that  $K^+$  and  $Na^+$  could both enter the mitochondria (Fig. 2E).

The light scattering response was clearly different between the  $K^+$  salts assayed. Mitochondria only contracted with KCl (Fig. 2B), whereas they swelled transiently with  $\geq 5$  mM KAc (Fig. 2E) and showed sustained swelling with  $KH_2PO_4$  (Fig. 2H). Under these conditions, mitochondrial volume was also assessed by the radioactive tracer method (see Materials and methods) with the following results (expressed as  $\mu\text{l}/\text{mg}$  mitochondrial protein  $\pm$  SEM;  $n=4$ ): control (before  $K^+$  salt addition) =  $1.75 \pm 1.8 \times 10^{-4}$ ; KCl =  $1.77 \pm 3.9 \times 10^{-4}$ ; KAc =  $2.15 \pm 7.2 \times 10^{-4}$ ;  $KH_2PO_4$  =  $2.54 \pm 3.4 \times 10^{-4}$ . In all three cases, increasing  $K^+$  concentration only slightly depolarized  $\Delta\Psi_m$  ( $\sim 5$ –10 mV) (Figs. 2C, F, and I).

### 3.2. Activation of $K^+$ fluxes through $K_{Ca}$ channels

We then analyzed the effect of NS11021, a novel activator of plasmalemma  $K_{Ca}$  channels [22], on mitochondrial  $K^+$  fluxes,  $\Delta\Psi_m$ ,

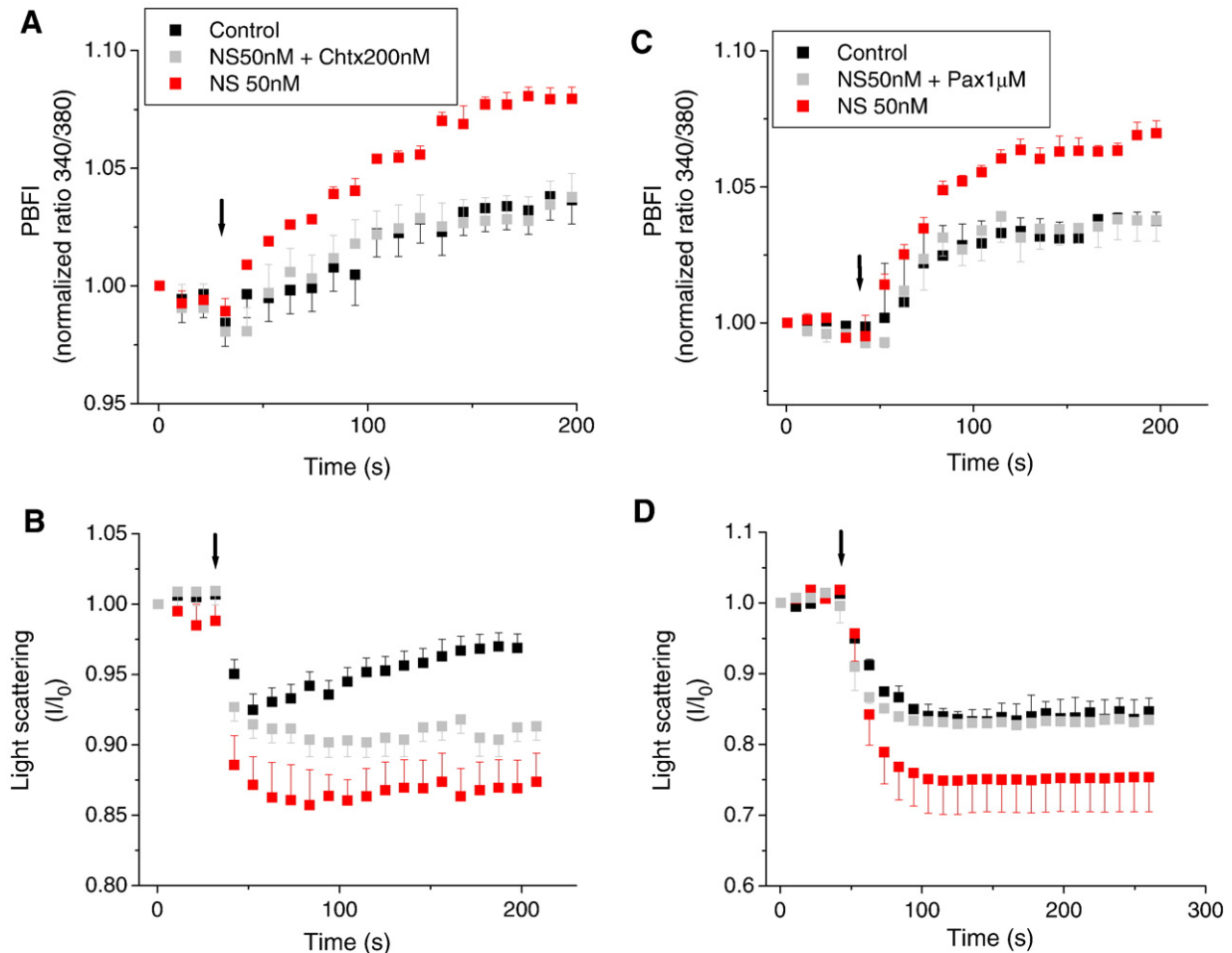


**Fig. 4.** Charybdotoxin and paxilline sensitivity of  $K^+$  uptake activation and mitochondrial volume increase elicited by NS11021. The effects of 200 nM ChTx (A, B) or 1  $\mu\text{M}$  paxilline (C, D) on  $K^+$  uptake (A, C) and mitochondrial swelling (B, D) in the presence of 50 nM NS11021 following the addition of 10 mM  $KH_2PO_4$  are shown. The PBFI ratio and  $90^\circ$  light scattering were monitored simultaneously. Arrows point to the time of the  $K^+$  salt addition. Representative results from two independent experiments with duplicates or triplicates within each are shown.

and volume, in the presence of the different  $K^+$  salts at near maximal  $K^+$  uptake rate (Fig. 3B). In the presence of  $KH_2PO_4$  or KAc, 50 nM NS11021 enhanced the rate of  $K^+$  uptake by 2.5-fold and increased mitochondrial volume, while a high  $\Delta\Psi_m$  was maintained ( $>190$  mV) (data not shown). In contrast, in the presence of KCl, 50 nM NS11021 increased  $K^+$  flux by only 30%, and no change in volume was observed, while  $\Delta\Psi_m$  was also maintained ( $>190$  mV).

Importantly, the NS11021 activation of  $K^+$  uptake was charybdotoxin (ChTx)- and paxilline (Pax)-sensitive; both of which are well-known  $K_{Ca}$  channel blockers [15]. Charybdotoxin (200 nM) blocked the increase in  $K^+$  flux (Fig. 4A) as well as the increase in matrix volume, at least partially (Fig. 4B) induced by the addition of 10 mM or 20 mM  $KH_2PO_4$  in the presence of 50 nM NS11021. Paxilline (1  $\mu$ M) blocked the activation of  $K^+$  flux (Fig. 4C) and the increase in volume (Fig. 4D) induced by 50 nM NS11021.

### 3.2. Selective and nonselective effects of NS11021 on mitochondrial respiration

The impact of selective activation of  $K_{Ca}$  channels upon respiration was evaluated by determining the effect of NS11021 on the RCR and the P/O ratio. The RCR (= state 3/state 4 respiration) was measured under the same conditions that an increase in  $K^+$  flux and mitochondrial volume were observed (Figs. 3 and 4). Fifty nanomolar

of NS11021 significantly increased the RCR by 70%, in the presence of 20 mM  $KH_2PO_4$  (Fig. 5A). In contrast, 1  $\mu$ M NS11021 significantly decreased the RCR. The P/O ratio in the presence of 50 nM NS11021 did not differ from the control but decreased in the presence of 1  $\mu$ M NS11021 (mean  $\pm$  SEM: control =  $2.14 \pm 0.19$ ; NS50nM =  $2.05 \pm 0.11$ ; NS1 $\mu$ M =  $1.48 \pm 0.11$ ;  $n = 3$ ).

In the presence of 10 mM KCl, the RCR was also higher with 50 nM NS11021, but this difference was not statistically significant; however, 1  $\mu$ M NS11021 still decreased RCR (Fig. 5C). Importantly, preincubation with 200 nM ChTx (Fig. 5B) or 1  $\mu$ M paxilline (not shown) prevented the effect of 50 nM, but not 1  $\mu$ M, NS11021 on RCR (with  $KH_2PO_4$ ), confirming that the effects of 50 nM NS11021 on  $K^+$  uptake, mitochondrial volume, and respiration were all mediated by mito $K_{Ca}$  channels.

Interestingly, the increase in RCR observed was due to a decrease in state 4 respiration rather than an increase in state 3, which was unchanged by 50 nM NS11021 (Fig. 5A, insets). One micromolar of NS11021 significantly increased state 4 respiration without affecting state 3 compared to the control (Fig. 5A, insets), accounting for the decrease in RCR. The decrease in state 4 observed in the presence of 50 nM NS11021 was abrogated by ChTx (Fig. 5B, inset). Furthermore, an acute decrease in the rate of state 4 respiration was registered upon addition of  $KH_2PO_4$  in the case of mitochondria preincubated with 50 nM NS11021 (Fig. 1C), in agreement with the increased RCR

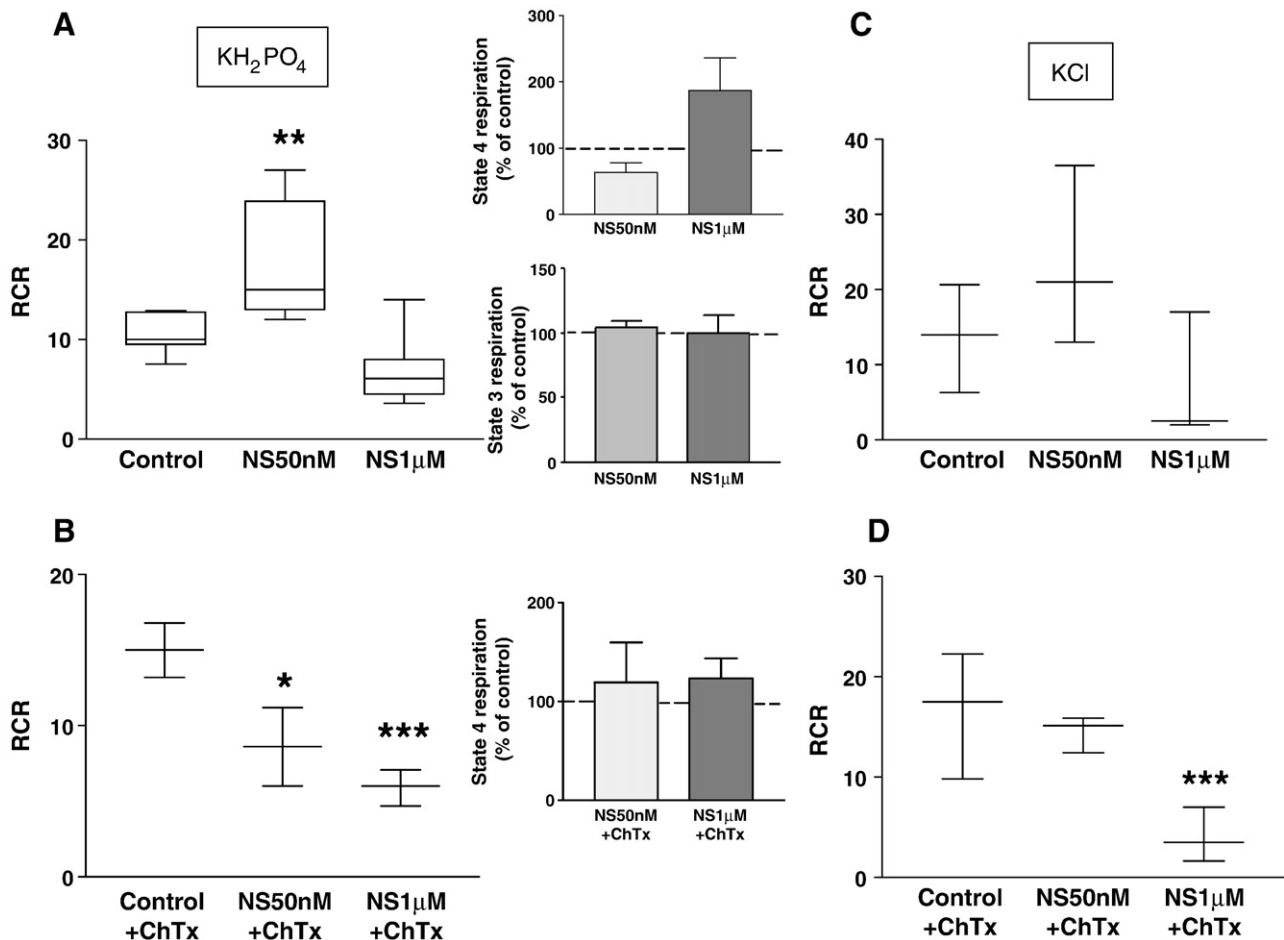


**Fig. 5.** Effects of NS11021 on mitochondrial respiration. Freshly isolated mitochondria from guinea pig heart were assayed for state 4 and state 3 mitochondrial respiration under the same conditions described in the legends of Figs. 1 and 2. The RCR (state 3/state 4) was calculated without (control) or with preincubation of 50 nM or 1  $\mu$ M NS11021 and 10 or 20 mM  $KH_2PO_4$  (A) or 10 or 20 mM KCl (C) without (A, C) or with (B, D) 200 nM ChTx. In panel A, the box plots depict the median (line), 25th and 75th percentile (box) and the minimum and maximum value (bars), whereas only the median with maximal and minimal values are represented in all other panels. Panel A: Control ( $n = 8$ , 4 experiments); NS50nM ( $n = 8$ ; 4 experiments); NS1 $\mu$ M ( $n = 8$ ; 4 experiments). Panel B: Control ( $n = 4$ ; 2 experiments); NS50nM ( $n = 4$ ; two experiments); NS1 $\mu$ M ( $n = 4$ ; 2 experiments). Panel C: Control ( $n = 4$ ; 2 experiments); NS50nM ( $n = 4$ ; 2 experiments); NS1 $\mu$ M ( $n = 4$ ; 2 experiments). Panel D: Control ( $n = 4$ ; 2 experiments); NS50nM ( $n = 4$ ; 2 experiments); NS1 $\mu$ M ( $n = 4$ ; 2 experiments).

described above (Figs. 5A and B).  $\Delta\Psi_m$  was not significantly depolarized by 50 nM NS11021 (Fig. 6A).

ChTx did not prevent the decrease in RCR induced by high concentrations of NS11021, in the presence of either  $\text{KH}_2\text{PO}_4$  or KCl (Figs. 5B and D). There was a larger decrease in RCR with 1  $\mu\text{M}$  NS11021 in the presence of ChTx, presumably because any beneficial effects of  $\text{K}_{\text{Ca}}$  channel activation were blocked, thus enhancing the nonspecific negative effect. Indeed, a decrease of  $\Delta\Psi_m$  from  $-193$  mV (control) to  $-160$  mV was observed when mitochondria were preincubated with 1  $\mu\text{M}$  NS11021, and further depolarization occurred upon addition of the  $\text{K}^+$  salts (Fig. 6A). An even larger collapse of  $\Delta\Psi_m$  was observed after preincubating with 2  $\mu\text{M}$  (Fig. 6A) or 5  $\mu\text{M}$  NS11021 (not shown).

Control experiments were carried out using NS13558, which bears an additional methyl group on the tetrazole moiety of the parent compound. This modification renders the compound inactive with respect to the activation of surface membrane  $\text{K}_{\text{Ca}}$  channels (data not shown). Importantly, 50 nM NS13558, in contrast with NS11021, did not increase  $\text{K}^+$  fluxes (Fig. 7A), nor did it improve RCR (Fig. 7B) with any of the  $\text{K}^+$  salts. NS13558 also did not increase volume or change  $\Delta\Psi_m$  at the 50 nM concentration (see Fig. S2, Supplementary data). However, micromolar amounts of NS13558 produced nonspecific effects similar to those of NS11021, such as marked  $\Delta\Psi_m$  depolarization and decreased RCR (Fig. 7B).

The effects of NS11021 were then compared with those of the artificial  $\text{K}^+$  ionophore valinomycin. Preincubation with valinomycin in the picomolar (pM) range, followed by addition of  $\text{KH}_2\text{PO}_4$ , also induced a moderate ( $\sim 10$  mV up to 100 pM Val) or more drastic

decrease of  $\Delta\Psi_m$  ( $\sim 30$  to 40 mV at  $>500$  pM Val; Fig. 6B), enhanced  $\text{K}^+$  influx (Fig. 6C) and high-amplitude swelling (Fig. 6D).  $\Delta\Psi_m$  was not depolarized by Val in the absence of  $\text{K}^+$  salts (Fig. 6B), but this was not true for NS11021 concentrations  $>1$   $\mu\text{M}$  (Fig. 6A), which depolarized  $\Delta\Psi_m$  even in the absence of  $\text{K}^+$ . The RCR was not affected by  $\text{Val} < 100$  pM; RCR decreased thereafter due to a significant increase in state 4 and a decrease in state 3 respiration after addition of the  $\text{K}^+$  salt (see Fig. S1, Supplementary data). These data indicate that it is the specific activation of  $\text{K}^+$  fluxes through  $\text{K}_{\text{Ca}}$  channels by low concentrations of NS11021 that improves energetic performance and that valinomycin cannot substitute for the effect.

#### 4. Discussion

The present work demonstrates that the specific activation of ChTx- or paxilline-sensitive  $\text{K}_{\text{Ca}}$  channels with NS11021 (at nanomolar concentrations) improves mitochondrial energetic performance and that this effect is correlated with enhanced  $\text{K}^+$  uptake and low-amplitude swelling without a large change in  $\Delta\Psi_m$ . Importantly, our findings (summarized in Fig. 8) also demonstrate that the inactive congener NS13558 did not show any of these effects. In contrast, micromolar concentrations of NS11021 or NS13558 significantly decreased RCR and the P/O ratio, independent of the mitochondrial  $\text{K}_{\text{Ca}}$  channel. Surprisingly, the increase in RCR was due to a decrease in state 4 respiration in response to activation of  $\text{K}^+$  flux, with similar state 3 respiration. In contrast, micromolar concentrations of NS11021 or NS13558 not only decreased RCR but also induced

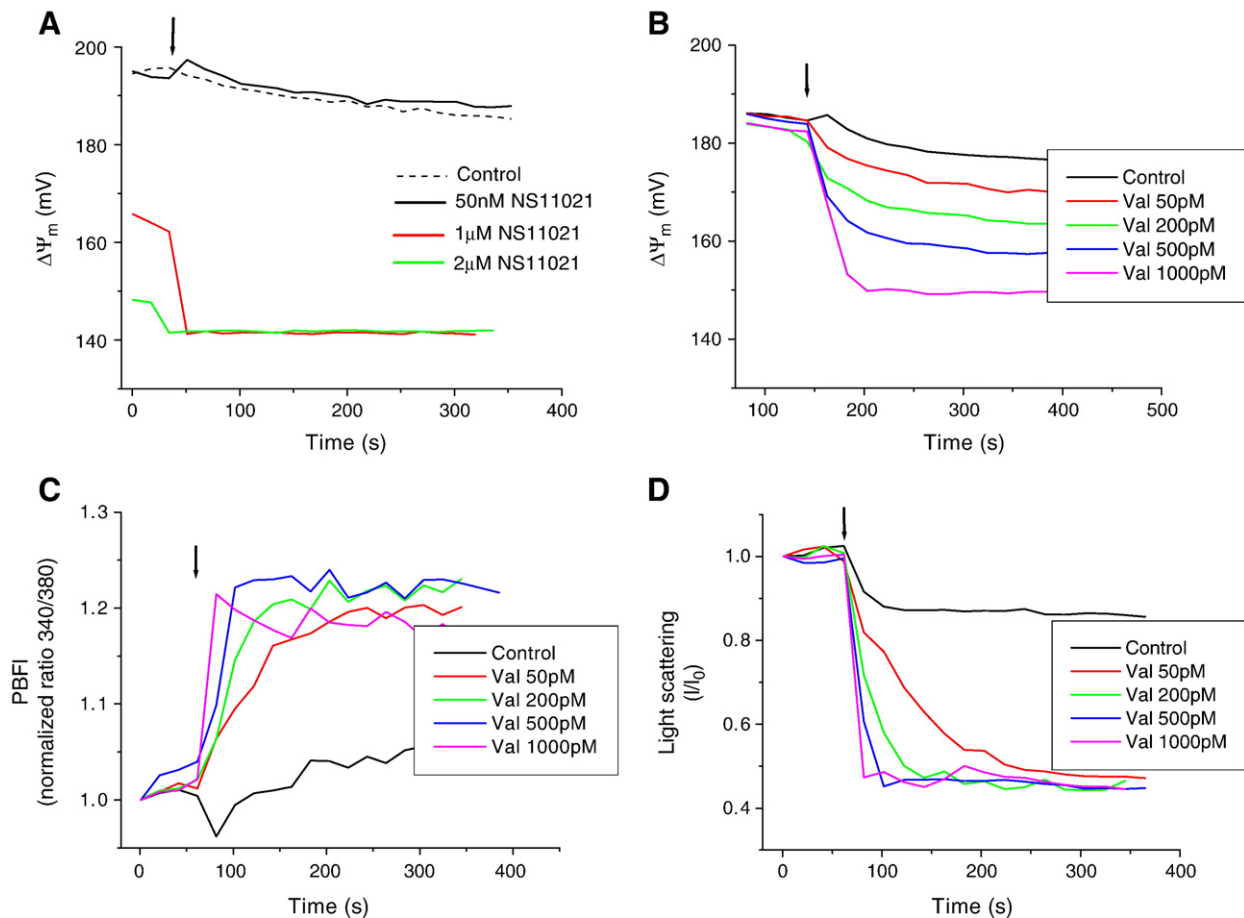


**Fig. 6.** Comparative effects of NS11021 and valinomycin before or after addition of  $\text{K}^+$  salt. Freshly isolated mitochondria from guinea pig heart were assayed as described in the legend of Fig. 2 without or with NS11021 (A) or valinomycin (B–D) preincubation within the 25 pM to 1 nM range (shown are 50 pM, 200 pM, 500 pM, 1 nM Val). Mitochondrial  $\Delta\Psi_m$ ,  $\text{K}^+$  flux, and volume were monitored as described in the legend of Fig. 2. Arrows point to the time of 10 mM  $\text{KH}_2\text{PO}_4$  addition.



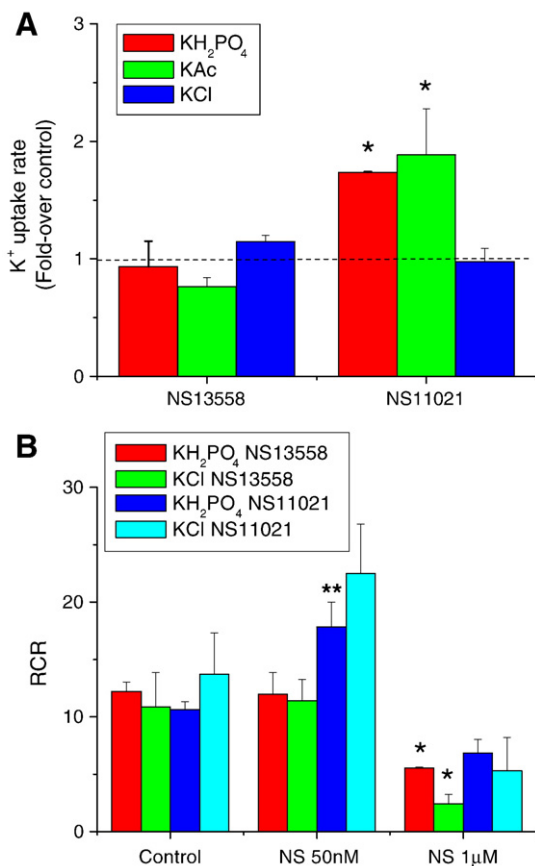


**Fig. 7.** Comparative effects of the  $K_{Ca}$  activator NS11021 and its inactive congener NS13558 on  $K^+$  fluxes and mitochondrial respiration. Freshly isolated mitochondria from guinea pig heart were assayed under similar conditions as described in the legends of Figs. 3 and 5. (A) The initial rates of  $K^+$  uptake after addition of 10 mM KCl, KAc, or  $KH_2PO_4$ , to state 4 mitochondria in the absence (control) or the presence of 50 nM or 1  $\mu$ M of NS13558 or NS11021. The PBF ratio, 90° light scattering, and  $\Delta\Psi_m$  were monitored simultaneously in duplicates. Shown are the  $K^+$  fluxes normalized to the control (absence of NS compounds) for each  $K^+$  salt, whereas the other variables are described in Fig. S2 of the Supplementary data. (B) Mitochondria were assayed for state 4 and state 3 respiration in triplicates, and the RCR (state 3/state 4) calculated without (control) or with preincubation of 50 nM or 1  $\mu$ M of NS13558 or NS11021, and 10 or 20 mM  $KH_2PO_4$  or 10 or 20 mM KCl.

depolarization of  $\Delta\Psi_m$  even in the absence of  $K^+$ , which was insensitive to  $K^+$  channel blockers. The latter nonspecific effect occurred in a concentration range similar to that used by others, when examining the behavior of NS1619, a related, but less potent,  $K_{Ca}$  channel opener [3,20]. The lack of effect of NS11021 on the P/O ratio (100  $\mu$ M ADP) indicates that the stoichiometry of ATP production as a function of  $O_2$  consumption is not substantially altered; therefore, we would not expect a large change in ATP synthesis with metabolic demand but would perhaps expect less energy wastage when respiration slows, for example, during conditions of ischemia when the mitochondria move closer to state 4. On the contrary, the nonspecific actions of the NS compounds decrease the P/O ratio and reduce metabolic efficiency.

#### 4.1. Volume regulation, energetic performance, and structural–functional coupling in mitochondria

Structural–functional coupling associated with mitochondrial energetics and volume regulation was described early on by Hackenbrock [37]. Based on electron microscopy data, he showed that the mitochondrial inner membrane/matrix compartment is organized as a network that undergoes geometric rearrangement from tightly packed (“condensed”), evident in mitochondria in state 3,

to an expanded (“orthodox”) lattice in state 4. Hackenbrock [37] observed low-amplitude swelling (10%–15% relative change) on addition of substrate (state 4 respiration), followed by mitochondrial contraction in the presence of ADP (state 4→state 3 transition). Moreover, these changes in volume occurred in association with substantial modifications in energetics, notably  $\Delta\Psi_m$ , redox, and  $O_2$  consumption. In the condensed state, it has been argued that matrix proteins are packed so tightly that the mobility of water is partially restricted [38] and its viscosity is ~15-fold higher than that of the cytosol [39]. Additionally, Hackenbrock suggested that the reticular proteic network of the matrix is physically continuous with the inner mitochondrial membrane, influencing its conformation and functions including ion and metabolite transport [37,40]. More recently, these ideas have been supported by electron tomographic imaging combined with cryo-microtomy techniques [41] further demonstrating that the transitions between orthodox and condensed conformations involves extensive remodeling of the cristae by fusion and fission mechanisms [42,43].

These observations have led to the idea that changes in mitochondrial volume and cristae structural organization could have an impact on oxidative phosphorylation; and enhanced substrate oxidation with matrix volume expansion has been demonstrated [13]. The present findings demonstrate that changes in  $K^+$  influx through mitochondrial  $K_{Ca}$  channels appear to be obligatory for the improvement in RCR. The beneficial effect was facilitated by permeant anions and preservation of  $\Delta\Psi_m$  was also important: this characteristic distinguished the positive effect of NS11021 from the nonspecific actions of the compound. Since the nonspecific actions were never, in our experiments, inhibited by selective channel inhibitors, they are also unlikely to be responsible for the cardioprotective actions of  $K^+$  channel openers.

The degree of anion permeability was directly correlated with the extent of mitochondrial volume increase and the decrease in state 4 respiration. In fact, in the presence of  $H_2PO_4^-$ , the volume increase initiated by  $K^+$  uptake was 45% larger, as compared with that obtained in the presence of  $Cl^-$ . However, the change in  $\Delta\Psi_m$  was small for all three anions after  $K^+$  addition (Fig. 2), suggesting that the cation, anion and water redistribution required to maintain charge balance [32] during adaptation of matrix volume, occurs without a significant change in electrochemical driving force.

Several mechanisms have been proposed to explain how small changes in volume could improve mitochondrial energetic performance, especially with respect to the activation of cardioprotective mitochondrial  $K^+$  channels [2,44,45]. Potential mechanisms include an optimization of the efficiency of nucleotide exchange by closer apposition of the inner and outer mitochondrial membranes [45], an increase in reactive oxygen species that trigger protective signaling pathways, and inhibition of glycogen synthase kinase-3  $\beta$  [46]. An enhanced ability of mitochondria to tolerate high ADP loads in the presence of  $K^+$  was also noted as an important protective factor linking  $K^+$  fluxes with matrix volume regulation [47]. The present findings suggest an additional novel response of mitochondria to the activation of mito $K_{Ca}$  channels – a decrease in state 4, but not state 3, respiration, resulting in an increase in RCR. The mechanism linking the increase in  $K^+$  flux, matrix volume, and the paradoxical decrease in state 4 proton leak will require further investigation. The folding and unfolding of mitochondrial matrix cristae are known to be a dynamic process, and our results suggest that  $K_{Ca}$ -mediated  $K^+$  uptake might alter the topology of the membrane, with concomitant changes in respiratory chain function. Consequently, we propose that this effect could reflect a structural reorganization of the mitochondrial inner membrane induced by the  $K^+$ -mediated increase in volume, perhaps through a mechano-sensitive ion channel controlling the proton leak across the membrane. This would imply that the changes in volume are coupled with changes in the tension on the membrane. Inte-



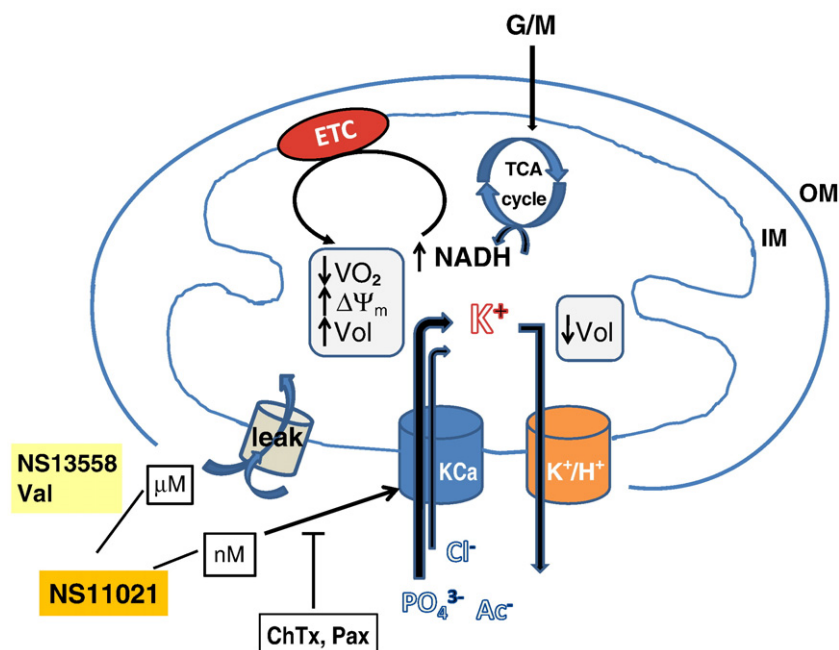


**Fig. 8.** NS11021 actions on mitochondrial energetics. NS11021 activation of  $\text{KCa}$  channel-dependent  $\text{K}^+$  influx (charybdotoxin- and paxilline-inhibitable), increases matrix volume in mitochondria energized with complex I substrates glutamate/malate (G/M) in the absence of ADP (state 4, low respiration, high  $\Delta\Psi_m$ , and NADH).  $\text{K}^+$  influx and mitochondrial volume are quickly balanced by the  $\text{K}^+/\text{H}^+$  antiporter, which expels the cation from the matrix. The specific activation of  $\text{K}^+$  flux through the  $\text{KCa}$  channel by NS11021 occurs in the nanomolar concentration range, whereas nonspecific ion leak occurs in the micromolar range. The inactive form NS13558 did not evoke  $\text{KCa}$ -specific actions but retained the nonspecific effects at micromolar levels. The scheme also highlights that the degree of  $\text{K}^+$  influx and the increase in volume is dependent upon the anion permeability ( $\text{H}_2\text{PO}_4^-$  and  $\text{Ac}^- > \text{Cl}^-$ ) and that the valinomycin-activated effects differ from those of the  $\text{KCa}$  channel. Key to symbols:  $\text{KCa}$ ,  $\text{Ca}^{2+}$ -dependent  $\text{K}^+$  channel (mito $\text{KCa}$ );  $\text{K}^+/\text{H}^+$ ,  $\text{K}^+/\text{H}^+$  antiporter; ETC, electron transport chain; ChTx, charybdotoxin; Pax, paxilline; IM, inner membrane; OM, outer membrane.

restingly, this type of system is present in bacteria, which involves the insertion of a mechano-sensitive channel to protect against osmotic shock, and the insertion pathway is evolutionarily conserved in chloroplasts and mitochondria [48]; however, no such mechano-sensitive channels have been identified in mitochondria thus far.

The  $\text{KCa}$ -specific effects of NS11021 on mitochondrial function were subtle when compared to the effects of the  $\text{K}^+$  ionophore valinomycin. While Val also enhanced the  $\text{K}^+$  uptake rate in a concentration-dependent manner, it induced a larger amplitude swelling. Low concentrations ( $<100$  pM) of Val only slightly depolarized  $\Delta\Psi_m$  ( $\sim 10$  mV) but high concentrations ( $>200$  pM) induced an abrupt depolarization when  $\text{KH}_2\text{PO}_4$  was added (this effect differed from the nonspecific effects of micromolar concentrations of NS11021, which depolarized  $\Delta\Psi_m$  even in sucrose medium in the absence of  $\text{K}^+$  salt) (Fig. 6). Val treatment did not decrease state 4 respiration at any concentrations tested in the range of 50 pM to 1 nM (see Fig. S1, Supplementary data). Taken together, the results obtained with Val and NS11021, at picomolar versus nanomolar concentrations, respectively, suggest that the mechanistic response to  $\text{K}^+$  transport induced by these two compounds is different. Alternatively, their differential effects on unitary  $\text{K}^+$  conductance could explain the different energetic responses. In addition, the effect of NS11021 to decrease state 4 respiration does not appear to be a feature of mitochondrial  $\text{K}_{\text{ATP}}$  channel openers, which dose-dependently increase state 4 respiration in a  $\text{K}^+$ -specific manner [49].

In summary, the present findings support the idea that the selective activation of mitochondrial  $\text{KCa}$  channels modulates  $\text{K}^+$  uptake and volume while maintaining  $\Delta\Psi_m$ . These properties are likely required to confer protection without compromising oxidative phosphorylation during recovery from metabolic stress. In contrast to other proposed mechanisms involving a slight uncoupling effect (increased respiration not coupled to ATP production), increased  $\text{K}^+$  flux through the  $\text{KCa}$  channel apparently decreases state 4 respiration, thus improving the respiratory control ratio of the mitochondria.

## Acknowledgements

The technical assistance of Agnes Sidor and Ling Chen is gratefully acknowledged. This work was supported by NIH grants P01HL081427 and R37HL54598, and The Novo Nordisk Foundation, The Aase and Ejnar Danielsen Foundation, and The Danish Medical Research Council (for M.G.).

## Appendix A. Supplementary data

Supplementary data associated with this article can be found, in the online version, at doi:10.1016/j.bbabbio.2009.08.002.

## References

- [1] K.D. Garlid, P. Dos Santos, Z.J. Xie, A.D. Costa, P. Paucek, Mitochondrial potassium transport: the role of the mitochondrial ATP-sensitive  $\text{K}^+$  channel in cardiac function and cardioprotection, *Biochim. Biophys. Acta* 1606 (2003) 1–21.
- [2] B. O'Rourke, Evidence for mitochondrial  $\text{K}^+$  channels and their role in cardioprotection, *Circ. Res.* 94 (2004) 420–432.
- [3] P. Bednarczyk, G.D. Barker, A.P. Halestrap, Determination of the rate of  $\text{K}^+$  movement through potassium channels in isolated rat heart and liver mitochondria, *Biochim. Biophys. Acta* 1777 (2008) 540–548.
- [4] A. Kaasik, D. Safulina, A. Zharkovsky, V. Veksler, Regulation of mitochondrial matrix volume, *Am. J. Physiol. Cell. Physiol.* 292 (2007) C157–C163.
- [5] G.P. Brierley, The uptake and extrusion of monovalent cations by isolated heart mitochondria, *Mol. Cell. Biochem.* 10 (1976) 41–63.
- [6] K.D. Garlid, *Chemiosmotic Theory*, Elsevier, 2004.
- [7] P. Bernardi, Mitochondrial transport of cations: channels, exchangers, and permeability transition, *Physiol. Rev.* 79 (1999) 1127–1155.
- [8] A.P. Halestrap, S.J. Clarke, I. Khaliullin, The role of mitochondria in protection of the heart by preconditioning, *Biochim. Biophys. Acta* 1767 (2007) 1007–1031.
- [9] F.G. Akar, M.A. Aon, G.F. Tomaselli, B. O'Rourke, The mitochondrial origin of postischemic arrhythmias, *J. Clin. Invest.* 115 (2005) 3527–3535.
- [10] G.C. Brown, Control of respiration and ATP synthesis in mammalian mitochondria and cells, *Biochem. J.* 284 (Pt. 1) (1992) 1–13.
- [11] A.P. Halestrap, The regulation of the matrix volume of mammalian mitochondria in vivo and in vitro and its role in the control of mitochondrial metabolism, *Biochim. Biophys. Acta* 973 (1989) 355–382.
- [12] A.M. Davidson, A.P. Halestrap, Liver mitochondrial pyrophosphate concentration

- is increased by  $\text{Ca}^{2+}$  and regulates the intramitochondrial volume and adenine nucleotide content, *Biochem. J.* 246 (1987) 715–723.
- [13] A.P. Halestrap, The regulation of the oxidation of fatty acids and other substrates in rat heart mitochondria by changes in the matrix volume induced by osmotic strength, valinomycin and  $\text{Ca}^{2+}$ , *Biochem. J.* 244 (1987) 159–164.
  - [14] G.C. Brown, M.D. Brand, Changes in permeability to protons and other cations at high proton motive force in rat liver mitochondria, *Biochem. J.* 234 (1986) 75–81.
  - [15] W. Xu, Y. Liu, S. Wang, T. McDonald, J.E. Van Eyk, A. Sidor, B. O'Rourke, Cytoprotective role of  $\text{Ca}^{2+}$ -activated  $\text{K}^+$  channels in the cardiac inner mitochondrial membrane, *Science* 298 (2002) 1029–1033.
  - [16] R.M. Douglas, J.C. Lai, S. Bian, L. Cummins, E. Moczydlowski, G.G. Haddad, The calcium-sensitive large-conductance potassium channel (BK/MAXI K) is present in the inner mitochondrial membrane of rat brain, *Neuroscience* 139 (2006) 1249–1261.
  - [17] M. Piwonska, E. Wilczek, A. Szewczyk, G.M. Wilczynski, Differential distribution of  $\text{Ca}^{2+}$ -activated potassium channel beta4 subunit in rat brain: immunolocalization in neuronal mitochondria, *Neuroscience* 153 (2008) 446–460.
  - [18] A. Szewczyk, W. Jarmuszkiewicz, W.S. Kunz, Mitochondrial potassium channels, *IUBMB. Life* 61 (2009) 134–143.
  - [19] D. Siemen, C. Loupatatzis, J. Borecky, E. Gulbins, F. Lang,  $\text{Ca}^{2+}$ -activated K channel of the BK-type in the inner mitochondrial membrane of a human glioma cell line, *Biochem. Biophys. Res. Commun.* 257 (1999) 549–554.
  - [20] D.V. Cancherini, B.B. Queliconi, A.J. Kowaltowski, Pharmacological and physiological stimuli do not promote  $\text{Ca}^{2+}$ -sensitive  $\text{K}^+$  channel activity in isolated heart mitochondria, *Cardiovasc. Res.* 73 (2007) 720–728.
  - [21] A. Kicinska, A. Szewczyk, Large-conductance potassium cation channel opener NS1619 inhibits cardiac mitochondria respiratory chain, *Toxicol. Mech. Methods* 14 (2004) 59–61.
  - [22] B.H. Bentzen, A. Nardi, K. Calloe, L.S. Madsen, S.P. Olesen, M. Grunnet, The small molecule NS11021 is a potent and specific activator of  $\text{Ca}^{2+}$ -activated big-conductance  $\text{K}^+$  channels, *Mol. Pharmacol.* 72 (2007) 1033–1044.
  - [23] L. Mela, S. Seitz, Isolation of mitochondria with emphasis on heart mitochondria from small amounts of tissue, *Methods Enzymol.* 55 (1979) 39–46.
  - [24] A.D. Beavis, R.D. Brannan, K.D. Garlid, Swelling and contraction of the mitochondrial matrix: I. A structural interpretation of the relationship between light scattering and matrix volume, *J. Biol. Chem.* 260 (1985) 13424–13433.
  - [25] A.L. Lehninger, Water uptake and extrusion by mitochondria in relation to oxidative phosphorylation, *Physiol. Rev.* 42 (1962) 467–517.
  - [26] H. Tedeschi, D.L. Harris, Some observations on the photometric estimation of mitochondrial volume, *Biochim. Biophys. Acta* 28 (1958) 392–402.
  - [27] R.C. Scaduto, L.W. Grotyohann, Measurement of mitochondrial membrane potential using fluorescent rhodamine derivatives, *Biophys. J.* 76 (1999) 469–477.
  - [28] A.P. Halestrap, P.T. Quinlan, The intramitochondrial volume measured using sucrose as an extramitochondrial marker overestimates the true matrix volume determined with mannitol, *Biochem. J.* 214 (1983) 387–393.
  - [29] H. Rottenberg, The measurement of membrane potential and  $\Delta\text{pH}$  in cells, organelles, and vesicles, *Methods Enzymol.* 55 (1979) 547–569.
  - [30] S. Bose, S. French, F.J. Evans, F. Joubert, R.S. Balaban, Metabolic network control of oxidative phosphorylation: multiple roles of inorganic phosphate, *J. Biol. Chem.* 278 (2003) 39155–39165.
  - [31] L. Packer, Metabolic and structural states of mitochondria: I. Regulation by adenosine diphosphate, *J. Biol. Chem.* 235 (1960) 242–249.
  - [32] D.G. Nicholls, S.J. Ferguson, *Bioenergetics* 3, Academic Press, London, 2002.
  - [33] G.P. Brierley, C.D. Stoner, Swelling and contraction of heart mitochondria suspended in ammonium chloride, *Biochemistry* 9 (1970) 708–713.
  - [34] M.W. Weiner, Mitochondrial permeability to chloride ion, *Am. J. Physiol.* 228 (1975) 122–126.
  - [35] G.P. Brierley, M. Jurkowitz, D.W. Jung, Osmotic swelling of heart mitochondria in acetate and chloride salts. Evidence for two pathways for cation uptake, *Arch. Biochem. Biophys.* 190 (1978) 181–192.
  - [36] F. Palmieri, The mitochondrial transporter family (SLC25): physiological and pathological implications, *Pflügers Arch.* 447 (2004) 689–709.
  - [37] C.R. Hackenbrock, Chemical and physical fixation of isolated mitochondria in low-energy and high-energy states, *Proc. Natl. Acad. Sci. U. S. A.* 61 (1968) 598–605.
  - [38] K.D. Garlid, The state of water in biological systems, *Int. Rev. Cytol.* 192 (2000) 281–302.
  - [39] E.A. Lopez-Beltran, M.J. Mate, S. Cerdan, Dynamics and environment of mitochondrial water as detected by  $^1\text{H}$  NMR, *J. Biol. Chem.* 271 (1996) 10648–10653.
  - [40] B.A. Scalettar, J.R. Abney, C.R. Hackenbrock, Dynamics, structure, and function are coupled in the mitochondrial matrix, *Proc. Natl. Acad. Sci. U. S. A.* 88 (1991) 8057–8061.
  - [41] J. Frank, T. Wagenknecht, B.F. McEwen, M. Marko, C.E. Hsieh, C.A. Mannella, Three-dimensional imaging of biological complexity, *J. Struct. Biol.* 138 (2002) 85–91.
  - [42] C. Frezza, S. Cipolat, O. Martins de Brito, M. Micaroni, G.V. Bezoussenko, T. Rudka, D. Bartoli, R.S. Polishuck, N.N. Danial, B. De Strooper, L. Scorrano, OPA1 controls apoptotic cristae remodeling independently from mitochondrial fusion, *Cell* 126 (2006) 177–189.
  - [43] C.A. Mannella, D.R. Pfeiffer, P.C. Bradshaw, Moraru II, B. Slepchenko, L.M. Loew, C.E. Hsieh, K. Buttle, M. Marko, Topology of the mitochondrial inner membrane: dynamics and bioenergetic implications, *IUBMB Life* 52 (2001) 93–100.
  - [44] K.D. Garlid, P. Paucek, Mitochondrial potassium transport: the  $\text{K}^+$  cycle, *Biochim. Biophys. Acta* 1606 (2003) 23–41.
  - [45] A.J. Kowaltowski, S. Seetharaman, P. Paucek, K.D. Garlid, Bioenergetic consequences of opening the ATP-sensitive  $\text{K}^+$  channel of heart mitochondria, *Am. J. Physiol. Heart. Circ. Physiol.* 280 (2001) H649–H657.
  - [46] M. Juhaszova, D.B. Zorov, S.H. Kim, S. Pepe, Q. Fu, K.W. Fishbein, B.D. Ziman, S. Wang, K. Ytrehus, C.L. Antos, E.N. Olson, S.J. Sollott, Glycogen synthase kinase-3 $\beta$  mediates convergence of protection signaling to inhibit the mitochondrial permeability transition pore, *J. Clin. Invest.* 113 (2004) 1535–1549.
  - [47] P. Korge, H.M. Honda, J.N. Weiss,  $\text{K}^+$ -dependent regulation of matrix volume improves mitochondrial function under conditions mimicking ischemia-reperfusion, *Am. J. Physiol. Heart. Circ. Physiol.* 289 (2005) H66–H77.
  - [48] S.J. Facey, S.A. Neugebauer, S. Krauss, A. Kuhn, The mechanosensitive channel protein MscL is targeted by the SRP to the novel YidC membrane insertion pathway of *Escherichia coli*, *J. Mol. Biol.* 365 (2007) 995–1004.
  - [49] G. Debska, A. Kicinska, J. Skalska, A. Szewczyk, R. May, C.E. Elger, W.S. Kunz, Opening of potassium channels modulates mitochondrial function in rat skeletal muscle, *Biochim. Biophys. Acta* 1556 (2002) 97–105.